formation and strongly reduces incorporation of uracil, while only slightly affecting growth. We therefore conclude that the process of induced morphogenesis we have described is mediated by *de novo* synthesis of RNA's.

ESRA GALUN
JONATHAN GRESSEL
Section of Plant Genetics, Weizmann Institute of Science, Rehovoth, Israel

References and Notes

1. M. Hayashi, S. Spiegelman, N. C. Franklin, S. E. Luria, *Proc. Nat. Acad. Sci. U.S.* **49**, 729 (1963).
2. R. H. Doi and R. Igarashi, *ibid.* **52**, 755 (1964); A. I. Aronson, *J. Mol. Biol.* **11**, 576 (1965).
3. V. G. Lilly and H. L. Barnett, *Physiology of Fungi* (McGraw-Hill, New York, 1951), p. 314; Y. Gutter, *Bull. Res. Counc. Israel 5D*, 273 (1957).
4. J. Horowitz and E. Chargaff, *Nature* **184**, 1213 (1959); J. Horowitz, J. J. Saukkonen, E. Chargaff, *J. Biol. Chem.* **235**, 3266 (1960).
5. S. P. Champe and S. Benzer, *Proc. Nat. Acad. Sci. U.S.* **48**, 532 (1962).
6. *Trichoderma viride* No. M 2042 was obtained from Y. Gutter, Volcani Institute for Agricultural Research, Rehovoth, Israel.
7. B. Rosen, *J. Mol. Biol.* **11**, 845 (1965).
8. E. Harbers, N. K. Chaudhuri, C. Heidelberger, *J. Biol. Chem.* **234**, 1255 (1959).
9. S. S. Cohen, J. G. Flaks, H. D. Barner, M. R. Loeb, J. Lichtenstein, *Proc. Nat. Acad. Sci. U.S.* **44**, 1004 (1958).
10. L. Bosch, E. Harbers, C. Heidelberger, *Cancer Res.* **18**, 355 (1958).
11. K. F. Chakraborty and H. S. Loring, *J. Biol. Chem.* **235**, 2122 (1960).
12. S. Naono and F. Gross, *Compt. Rend.* **250**, 3889 (1960).
13 F. B. Salisbury and J. Bonner, *Plant Physiol.* **35**, 173 (1960); J. Bonner and J. A. D. Zeevaart, *ibid.* **37**, 43 (1962).
14. S. Katz and D. G. Comb, *J. Biol. Chem.* **298**, 3065 (1963).
15. The capable technical assistance of Cezar Tabbak and Dina Heller is gratefully acknowledged. 5-Fluorouracil was a gift of F. Hoffman-La Roche and Co.

8 December 1965

Virus Induction of Osteosarcomas in Mice

Abstract. *A virus extracted from an osteosarcoma of a mouse produces similar tumors when injected into newborn mice. The original tumor appeared spontaneously in an untreated CF1 male. The time between inoculation with virus and detection of bone sarcoma has been as short as 23 days.*

Because of growing evidence from other laboratories that some mouse tumors are caused by virus (*1*), we began a search for a viral agent that might be associated with osteogenic sarcomas in CF1 mice.

So far we have examined seven radiation-induced and four spontaneous osteosarcomas for evidence of virus by use of a modification of the method developed by Gross for isolating a leukemogenic agent from AK mice (*2*). Definite oncogenic activity has been found in an extract prepared from one of the spontaneous bone tumors.

The osteosarcoma from which the active agent was extracted appeared in a 260-day-old stock male mouse of the CF1/Anl strain. The tumor, which involved the 10th, 11th, and 12th thoracic vertebrae and the 12th rib (Fig. 1*A*), was removed under sterile conditions, ground in a cold mortar, and diluted with about five parts saline. A portion of the resulting cell suspension was injected into a litter of 12-day-old CF1 mice, and the remainder was centrifuged at 2500 rev/min for 10 minutes at 0°C (International centrifuge, model PR-2). The supernatant was centrifuged again for 20 minutes at 3300 to 3500 rev/min (approximately 1500*g*), and the resulting supernatant was injected subcutaneously into a newborn litter of CF1 mice and intraperitoneally into a litter that was 33 days old.

One of the mice that had received the extract on the day of birth died with an osteosarcoma of the cervical spine 280 days later. At 337 days a large tumor mass extending from the lower thoracic to the midlumbar spine was observed in another mouse of the same litter (Fig. 1*B*). An extract of this tumor was prepared as before and injected subcutaneously into four newborn litters of CF1 mice. A hard mass was observed on the back of one of the recipients when it was 67 days old, and 4 days later four more of the mice, belonging to three of the litters, had palpable bone tumors.

These four mice were killed at 71 days of age, and each was found to have two osteosarcomas. Five of the eight tumors were in the spine, two were in ribs, and one was in a humerus. The combined tumors were extracted, and a portion of the extract was put through a 0.45-μ, HA type, Millipore filter. Four newborn litters were inoculated subcutaneously, two with the extract and two with the cell-free filtrate. The first tumor was noted at 35 days in a mouse that received extract and at 61 days in a mouse that received filtrate. The latter animal had osteosarcomas in the sternum, first lumbar vertebra, right ilium, and right tibia when it was killed at 70 days of age.

The results obtained in one line of passage from the first extraction on 11 March 1963 to 11 March 1965, are summarized in Fig. 2. In each case 0.1 ml of material was injected either under the skin of the back or into the peritoneal cavity of CF1 mice. After the third passage only filtrates were used, and tests of the procedures showed the filters to be impervious to *Escherichia coli*. The chart includes all mice that survived to weaning age; preweaning mortality was somewhat higher than among undisturbed litters.

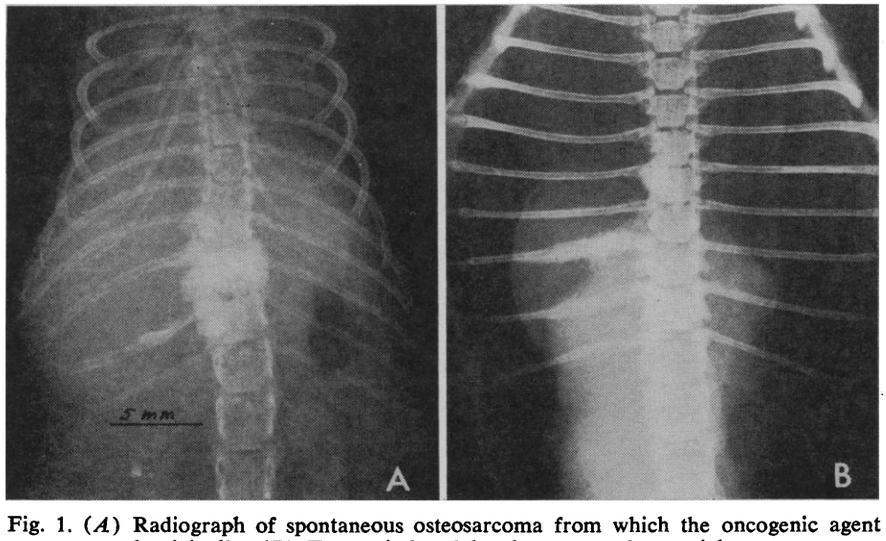

Fig. 1. (*A*) Radiograph of spontaneous osteosarcoma from which the oncogenic agent was extracted originally. (*B*) Tumor induced by the extracted material.

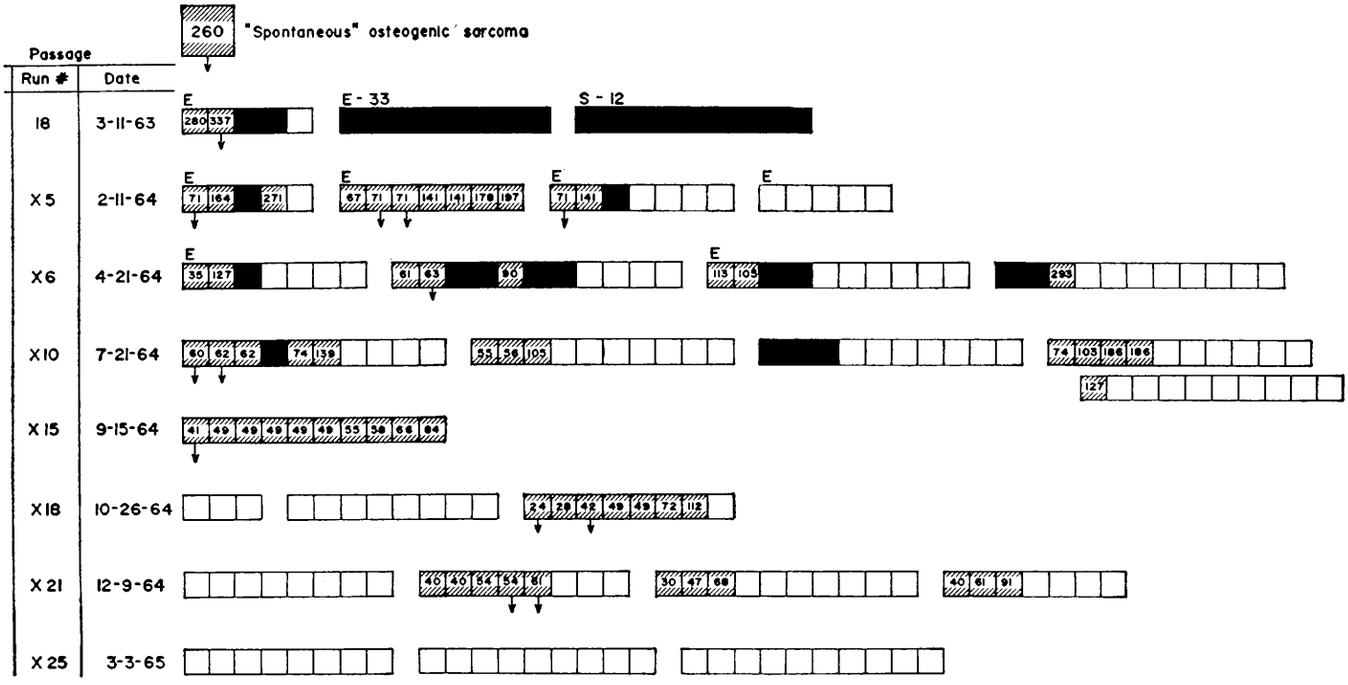

Fig. 2. Summary of 2 years' experience (ending 11 March 1965) along one line of passage. Each square represents a mouse, and joined squares represent littermates. The numbers in the shaded squares represent the age in days when the tumor was detected. The black represents mice that died without bone tumors. White squares represent living mice without (detected) bone tumors. All litters received filtrate except those marked *E* (extract) or *S* (cell suspension), and all were inoculated on the day of birth except two in the first passage (12 and 33 days old). Arrows designate donors of material for the next passage. In the X10 run there were five litters, the fifth being shown just beneath the fourth.

The time to the appearance of the first tumor decreased from 280 days in the first passage to 67 days in the second passage and to only 35 days in the third passage. Since then a few tumors have been palpated earlier, even at 23 days. The rapid appearance of an osteosarcoma in one member of a litter usually is followed rather soon by the appearance of tumors among other members of that litter. However, littermates are not always equally sensitive. For example, in the first litter of the second passage, three of the five mice have had bone tumors, but the time of appearance ranged from 71 to 271 days. One member of the litter died without tumor at 243 days, and one is still alive, apparently without tumor, 540 days after inoculation.

Some entire litters seem to be resistant to the oncogenic activity of the inoculum; however, some are particularly sensitive, such as the one that was used in the fifth passage, where each of the ten members had bone sarcoma by 84 days, and most of them had more than one tumor at death (Fig. 3).

During the 2-year period, 22 passages were made from the original

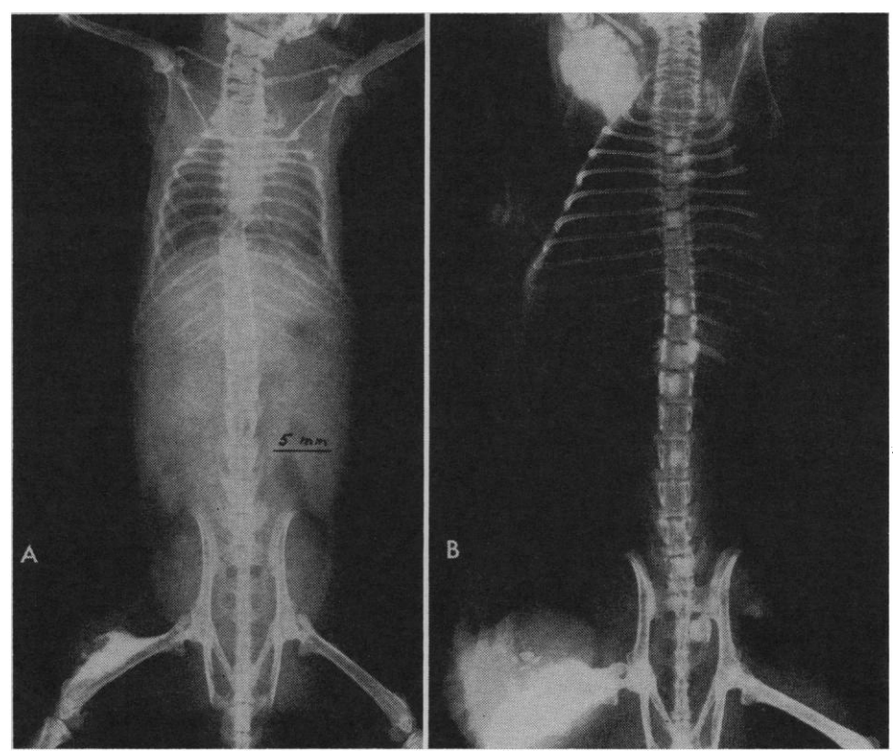

Fig. 3. Radiographs of a fifth-passage mouse. (*A*) Osteosarcoma of femur 58 days after inoculation. (*B*) Osteosarcomas of scapula, 13th thoracic vertebra, 2nd sacral vertebra, femur, and pubis at autopsy 106 days after inoculation. Tumors were also present in each humerus and the sternum. Several radiopaque areas in the thoracic and lumbar spine might be neoplastic.

osteosarcoma. Although more than half of the inoculated mice were still alive on 11 March 1965, 21.4 percent already had malignant bone tumors in contrast to the normal incidence in the CF1 strain of 1 to 2 percent. Other diseases have been rare among these mice, and there has been no indication that tumors of any other kind have been produced by the injection of extracts and filtrates from the osteosarcomas. Most of the animals that died without bone tumors were males injured in fights with cage mates.

The radiographic appearance of the tumors has not changed with successive passages. Proliferative activity seems to begin at the periosteum, and growth proceeds peripherally with deep cortical bone becoming involved relatively late. Microscopic appearance, also, has remained the same. Individual tumors usually show considerable histologic variation from region to region. Cell types range from fibroblasts to giant cells and osteocytes, and wide differences occur in the amount of osteoid and in the degree of ossification (Fig. 4).

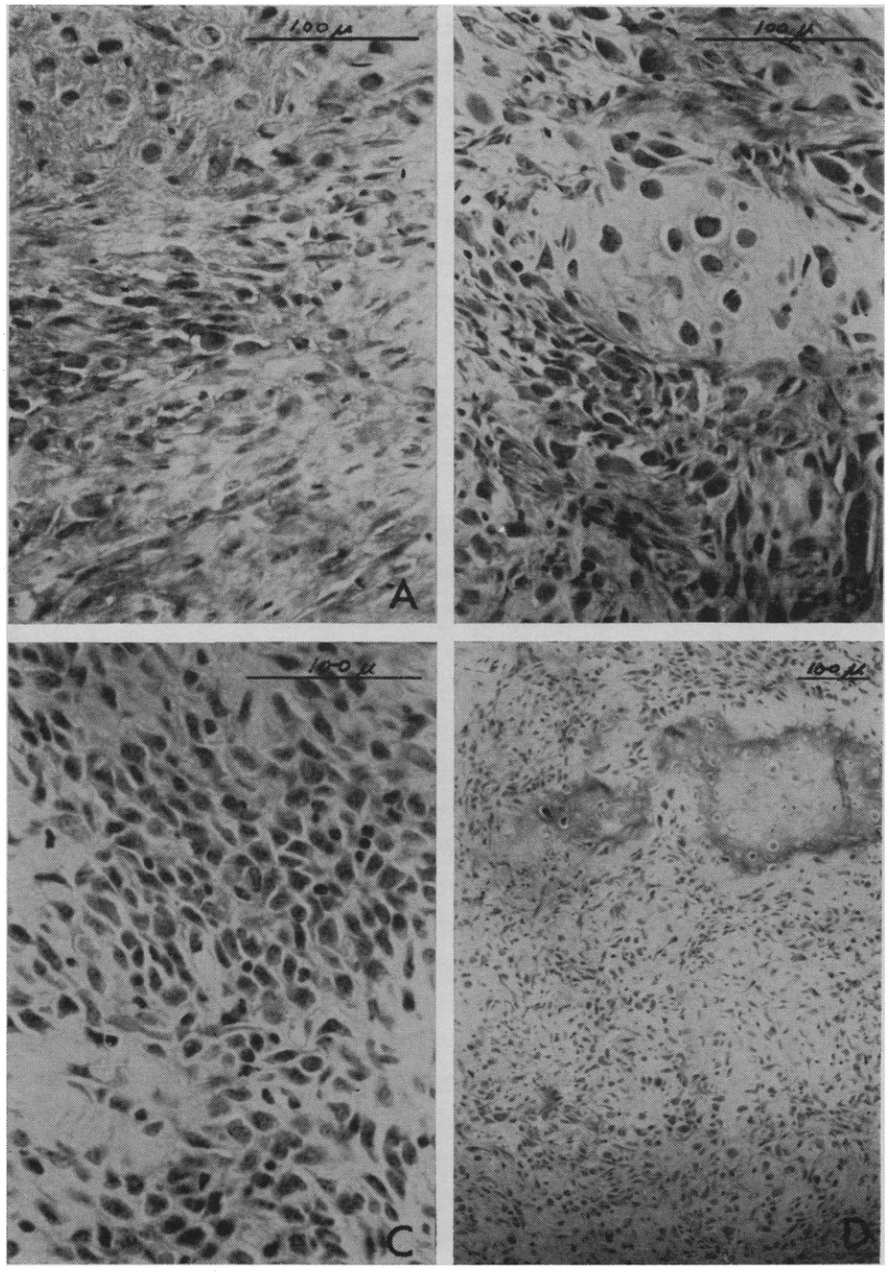

Fig. 4. (*A*) Photomicrograph of the original, spontaneous osteosarcoma, showing diversity of cells and matrix. (*B*) Osteosarcoma of ribs in a fifth-passage mouse 131 days after inoculation. (*C*) Osteosarcoma of sternum in a sixth-passage mouse 74 days after inoculation. (*D*) Tumor node in diaphragm of a sixth-passage mouse 55 days after inoculation.

Electron-microscopic examination of extracts and filtrates prepared from tumors of inoculated animals has shown tailed viral particles similar in size and morphology to some known murine oncogenic viruses (*3*). The particles also have been found in pellets that were formed by centrifuging extracts at 30,000 rev/min (average of 57,300*g*) for 60 minutes in a Spinco ultracentrifuge, and osteosarcomas have developed in mice inoculated with a portion of this same material.

Although this new agent resembles other murine oncogenic viruses, it differs from those described in that it produces only malignant bone tumors. The SE polyoma virus, which has caused a few osteogenic sarcomas, primarily produces a variety of soft tissue tumors (*4*). Serum from our tumor-bearing animals did not contain polyoma virus antibody.

Possibly the experiences of Pybus and Miller with bone tumors in mice were due to the same, or a similar, virus (*5*). By rigorous inbreeding of the progeny of tumor-bearing mice, they produced a line in which the incidence of bone tumors was increased tenfold over that found in the parent stock. Histologic type included osteoma, osteosarcoma, osteosarcoma with giant cells, and chondroosteosarcoma. They attributed their results to an inherited tendency on the part of the mice to develop bone tumors. However, since their mouse line ultimately lost this tendency, the disease might have had an infectious instead of a genetic basis.

For purposes of identification, the oncogenic agent isolated from the CF1 osteosarcoma has tentatively been named the FBJ virus (*6*).

MIRIAM P. FINKEL
BIRUTE O. BISKIS
PATRICIA B. JINKINS
Experimental Radiation Pathology, Argonne National Laboratory, Argonne, Illinois

References and Notes

1. L. Gross, *Oncogenic Viruses* (Pergamon, New York, 1961).
2. ———, *Proc. Soc. Exp. Biol. Med.* **76**, 27 (1951).
3. A. J. Dalton, F. Haguenau, J. B. Moloney,

J. Nat. Cancer Inst. **29**, 1177 (1962); R. F. Zeigel and F. J. Rauscher, *ibid.* **30**, 207 (1963); E. deHarven and C. Friend, *Virology* **23**, 119 (1964); J. A. Sykes, C. E. Grey, M. Scanlon, L. Young, L. Dmochowski, *Texas Rep. Biol. Med.* **22**, 609 (1964).
4. S. E. Stewart, B. E. Eddy, M. F. Stanton, *Can. Cancer. Conf.* **3**, 287 (1958).
5. F. C. Pybus and E. W. Miller, *Amer. J. Cancer* **33**, 98 (1938); *Brit. Med. J.* **1**, 1300 (1938); *Amer. J. Cancer* **34**, 248, 252 (1938); *ibid.* **40**, 47, 54 (1940).
6. Performed under the auspices of the USAEC.

1 November 1965

Fluorescent Tracer: Transport in Distance and Depth in Beach Sands

Abstract. *Foreshore tidal-cycle transport of sediment along a beach profile can be traced in distance and depth by the use of fluorescent pigments. Sediment cores are obtained from locations on the profile, dyed in horizontal segments, and returned to their original positions in the beach. Analyses of flood- and ebb-tide samples of sediment reveal the pattern of littoral zone sedimentation.*

Investigations of sediment transport currently employ two basic injection and sampling procedures (*1*). In the space-integration method, counts of tracer particles over a sampling grid reveal the pattern of particle distribution, with the time-rate of change indicated by repeated sampling without replacement of tracer. The time distribution of tracer particles is determined, in the time-integration method, by sampling along a section transverse to the flow. Both techniques are limited to essentially surface transport along the length and breadth of the area being studied. The depth of foreshore erosion has been determined by placing vertical columns of tracer-labeled sediment in the beach (*2*).

A new procedure was devised in connection with a recent beach study, by which the sequence of tidal-cycle scour, transport, and deposition of particulate tracer grains can be followed along the beach profile; quantitative measurements of depth and particle numbers can also be obtained. The method thus adds a third dimension, that of depth, to the established sediment-transport techniques.

The technique was tested on sandy pocket beaches at Indian Harbour and Smith Cove, Guysborough County, Nova Scotia. Confined by headlands, incoming waves are refracted so as to break normal to the shoreline, thus minimizing sediment transport along the length of the beach.

At low water preceding the period of observation, two 6-cm-diameter cores of sediment were taken from the beach: one at the upper swash limit, and the other at mid-foreshore along the same profile. Small auxiliary cores were also taken from the same sites. The top 12 cm of sediment in the two larger, plunger-type, core tubes was removed in three equal horizontal increments. The six segments of sand thus obtained were dyed with different fluorescent colors by the method of Yasso (*3*). The segments of coated particles were then returned to the core tubes in their original positions to preserve the character of the layers in the beach. The mid-foreshore tracer core was designated X, the colored segments being blue, yellow, and red from the top down; the swash-limit tracer core was designated Y, the colors from top to bottom being pink, green, and orange (Fig. 1).

At low water on the day of observation, the tracer cores were returned to their original positions. Thin metal guide rods were driven into the beach 50 cm to each side of the tracers and their exposed heights were recorded. During the tidal cycle the beach profile adjacent to the tracer area was measured hourly (*4*); as the tide rose the exposures of guide rods above the sand-water interface were measured (*5*).

When tracer-core X was located in the lower portion of the flood-tide swash-backwash zone, samples A, B, C, and D were taken: the first three in core tubes with an inside diameter of 4.5 cm; the last in a 230-g container. The procedure was similar in obtaining samples E, F, G, and H during the ebb when tracer-core Y became located in a comparable position. In both instances the upper sample core (A–E) was located just seaward of the then-prevailing upper swash limit; the middle sample core (B–F), at the tracer-core site in the lower swash-backwash zone; the lower core (C–G), in the breaker zone; and the container sample (D–H), in the shoaling wave zone beyond the base of the step, as in Fig. 2 and (*6*).

These procedures were followed twice at the Smith Cove beach and four times at the beach at Indian Harbour.

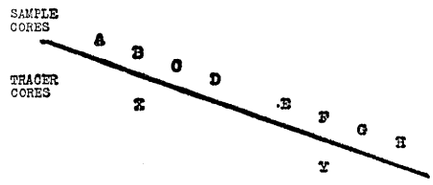

Fig. 1. Designation of sources of tracer and sample cores.

Hourly profiles were plotted for each tidal cycle, and surface-level changes at the guide rods were calculated. Analyses of grain-size distribution were made for each 4-cm increment of the small auxiliary cores that were taken when the sediments to be dyed were cored.

Each core sample, A, B, C, E, F, and G, was divided into two equal horizontal increments designated 1 and 2 from the top down; these were 3 to 5 cm in thickness, depending on the length of the core. Container samples D and H were split in a sediment-sample divider to make their volumes of the same order of magnitude as the other sample segments. Analyses of grain-size distribution were then made for each sample, and the number of particles of each fluorescent color in each size range in the samples was recorded. Thus, for each increment in depth of the core samples, and for the container samples, the grain-size and tracer-particle distributions were obtained and tabulated.

The plotted profiles and surface-level changes at the guide rods, together with visual observation of the tracer cores and sample cores, support the tidal-cycle sequence of phases of initial deposition, scour, and step deposition outlined by Strahler (*6*). A pattern of littoral-zone tidal-cycle sedimentation may be developed from the tabulation of data on grain-size and tracer-particle distribution, based

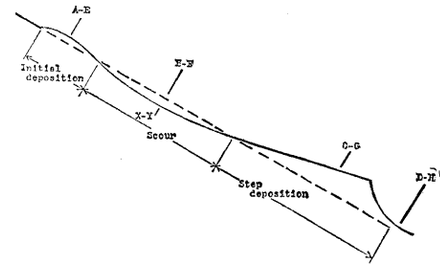

Fig. 2. Detail of sources of sample cores at time of sampling.